JOURNAL OF MATERIALS SCIENCE 32 (1997) 583–587

Electrical and mechanical properties of ZrO_2(2Y)/TiN composites and laminates made from these materials

KENRO SHIBATA, RIKIYA SATO, MASARU YOSHINAKA, KEN HIROTA, OSAMU YAMAGUCHI
Department of Molecular Science and Technology, Faculty of Engineering, Doshisha University, Kyoto Tanabe 610-03, Japan

High density composites with the compositions of ZrO_2(2Y):TiN = 40:60 and 70:30 mol% have been fabricated by hot isostatic pressing for 2 h at 1500 °C and 196 MPa. The electrical resistivities (ρ) of the two composites are very different; showing metallic behaviour in the first case and insulating behaviour in the latter case. These properties are highly dependent on the sample texture. Laminated materials with compositions of ZrO_2(2Y)/TiN = (40:60)/(70:30)/ (40:60) mol % have been prepared by hot isostatic pressing. The electrical resistivities in the perpendicular and parallel to the interface directions have been determined to be $\rho_\perp \approx 1 \times 10^9$ and $\rho_\parallel \approx 1 \times 10^{-6}\,\Omega\,m$, respectively. A residual stress of as much as $\approx$150 MPa is induced in the interfaces. The fracture toughness is greatly affected by the residual stress.

1. Introduction

Titanium nitride TiN, is an intermetallic compound, which finds use in highly refractory cermets employed in the melting of metals and also as a component of superhard cutting tools. The most common fabrication methods for producing dense TiN ceramics are conventional sintering and hot pressing in the presence of additives such as metallic Co or Ni [1, 2]. These additives play an important role in promoting densification but cause the precipitation of secondary phases at grain boundaries. Yamada *et al.* [3, 4] have fabricated pure dense TiN ceramics using high pressure hot pressing and also hot isostatic pressing and evaluated the sample microstructures, thermal conductivities, and Vickers hardness. Themelinm and Boncobva [5] studied the densification of pure TiN powder and reported that the fracture toughness and bending strength of hot isostatically pressed (1600 °C/180 MPa) TiN ceramics (99.3% of theoretical density) were 5 $MPa \cdot m^{1/2}$ and 550 MPa, respectively. On the other hand, the fracture toughness of chemically vapour-deposited TiN films was determined to be 3.7 $MPa \cdot m^{1/2}$ [6]. The main disadvantage of this material, as well as of almost all intermetallic compounds, is an inherent lack of toughness. It cannot therefore be employed by itself as a structural material but instead it needs to be reinforced in order to improve its mechanical properties. It has been previously reported that ZrO_2(2Y) is a highly praising reinforcement material for TiN [7]. In the present study, the electrical conductivities of ZrO_2(2Y):TiN = 40:60 and 70:30 mol % composites were found to drastically change from metallic in the former system to insulating behaviour in the latter composite (Fig. 1). These results suggest that laminated materials, consisting of metallic/insulating composites, can be expected to exhibit interesting properties. Little attention has been paid to the fabrication and properties of laminates containing composites of ceramics and intermetallic compounds. Laminated materials with the compositions of ZrO_2(2Y)/TiN = (40:60)/(70:30)/(40:60) mol % have been successfully fabricated by hot isostatic pressing. The purpose of this study is to evaluate the electrical and mechanical properties of the monolithic composites and the laminated materials.

2. Experimental procedure

Powders of ZrO_2 containing 2 mol % Y_2O_3 (Sumitomo Osaka Cement Co. Ltd.) and TiN (Japan New Metals Co. Ltd.) were used as the starting materials. The ZrO_2(2Y) was of high purity (99.97%) and had an average particle size of 0.023 μm. The purity of the TiN with an average particle size of 1.47 μm was 96.68%. The impurities were 1.82% carbon and 1.5% oxygen. Two compositions, denoted A and B, were chosen for this study (Table 1). Appropriate amounts of both starting powders were mixed for 20 h by wet-ball-milling on ethanol with zirconia balls in a polyethylene pot and the powders were then dried at 80 °C under reduced pressure. The mixed powders were calcined for 1 h at 1000 °C in a nitrogen atmosphere.

Monolithic composites and laminated materials were fabricated by hot isostatic pressing (HIPing) with argon gas acting as the pressure-transmitting medium.

0022–2461

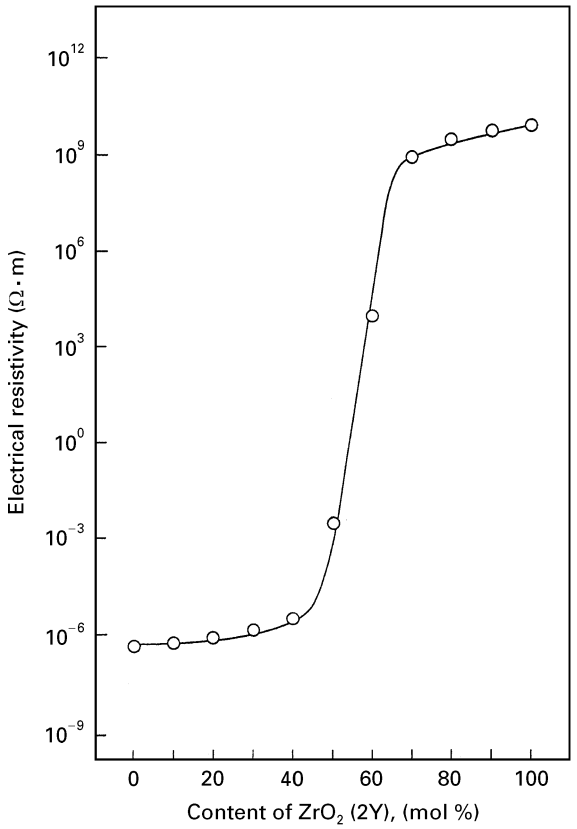

Figure 1 Electric resistivity of the composites as a function of ZrO_2 addition.

TABLE I Chemical composition of the starting powders and selected properties of the composites

Starting powder	Composition ZrO_2(2Y)/TiN (mol %)	Bulk density (g cm^{-3})	Relative density (%)	Grain size (μm)	
				ZrO_2(2Y)	TiN
A	40:60	5.74	99.5	0.23	1.5
B	70:30	5.93	99.7	0.23	1.5

Before HIPing, the calcined powders A and B were pressed into pellets at 147 MPa. The A/B/A assemblies were prepared by stacking the appropriate pellets in the correct order. These assemblies were then isostatically cold pressed at 196 MPa. The green compacts, covered with boron nitride powder, were sealed in a Pyrex-glass tube under vacuum. The HIPing conditions were as follows: a heating rate of 400 °C per h; an increasing pressure rate of ≈180 MPa per h above 800 °C; and sintering for 2 h at 1500 °C under a pressure of 196 MPa.

The bulk densities, after lapping with a diamond powder, were measured by the Archimedes method. The phases present in the polished surfaces were identified by X-ray diffraction (XRD) analysis using Ni-filtered CuK_α radiation. Scanning electron microscopy (SEM) was utilized for microstructural observations on both the fractured and polished surfaces. The electrical resistivity (ρ) was measured at 1 kHz by a two-probe technique using an impedance analyser. Test samples ($3 \times 12 \times 20$ mm) for the mechanical measurements were cut from the sintered bodies with a diamond saw and were lapped with a diamond paste. The fracture toughness (K_{IC}) measurements were made using the microindentation technique [8, 9] with a 196 N load. The three-point bending strength was measured with a 16 mm span and a crosshead speed of 0.5 mm per min.

3. Results and discussion

3.1. Characterization of the monolithic composites

XRD analysis showed that the as-received ZrO_2(2Y) powder contained a mixture of tetragonal (t) and monoclinic (m) ZrO_2 phases; the t:m ratio calculated from the Garvie and Nicholson equation [10] was 45:55 vol %. However, the ZrO_2 particles in the composites consisted of almost all t-ZrO_2. No crystalline phases other than TiN and ZrO_2 were observed in the composites. It should be noted that large amounts of t-ZrO_2 were present in the composites. This suggests that the ZrO_2 particles were below the critical size, for transformation from tetragonal to monoclinic symmetry during cooling, and therefore they remained as metastable t-ZrO_2. In fact, as will be described in detail later, the average grain size of the ZrO_2 in the composites was < 0.25 μm. The transformation of t- to m-ZrO_2 depends on a critical size which is closely related to the Young's modulus of the matrix [11]. The Young's moduli of TiN and ZrO_2(2Y) are ≈400 [12] and 207 MPa [13], respectively. In view of the fact that the value of the former is ≈1.9 times higher than that of the latter, it can be assumed that the t-ZrO_2 particles were retained in the composites.

Table 1 shows the bulk and relative densities of the composites. As the theoretical density of m-ZrO_2(2Y) was unknown, a value of 5.829 g cm^{-3} was estimated by assuming that the t- → m-ZrO_2 transformation involves a 4.4% increase in volume [14] and this increased volume was used in the calculation of the relative densities. The theoretical densities of TiN and t-ZrO_2(2Y) were assumed to be 5.43 [3] and 6.085 g cm^{-3} [15], respectively. The composites A and B reached 99.5 and 99.7% of the theoretical density, respectively. Thus, well-densified TiN–ZrO_2(2Y) composites could be prepared by HIPing. Fig. 2(a and b) shows SEM photographs of the fracture surfaces of the composites. They show microstructures that consist of large TiN grains and small ZrO_2(2Y) grains. The average grain sizes, determined directly by SEM observations, are listed in Table 1. The grain sizes of TiN and ZrO_2 were 1.5 and 0.23 μm, respectively, regardless of the starting composition. No grain growth of TiN occurred. The nature of the dispersion could not be clearly resolved by the above observation. However, a backscattered electron image on the polished surfaces showed the dispersion to be homogeneous (Fig. 3(a and b)). Significant information regarding the composite textures will be described later, in connection with the electric resistivities of composites.

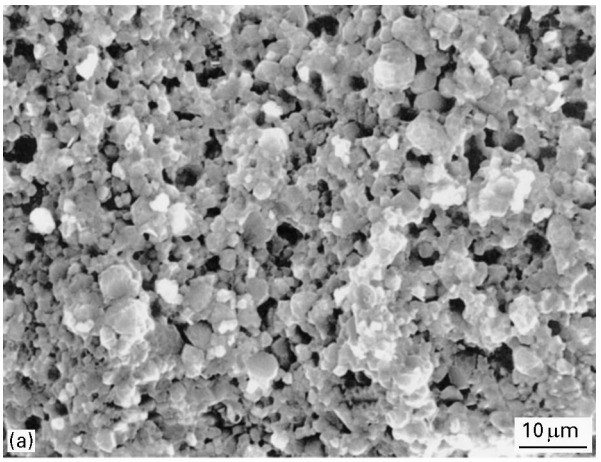

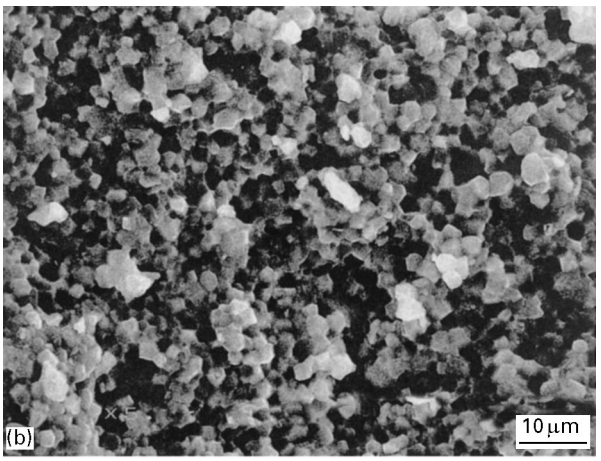

Figure 2 SEM photographs of fractured surfaces of (a) composite A and (b) composite B.

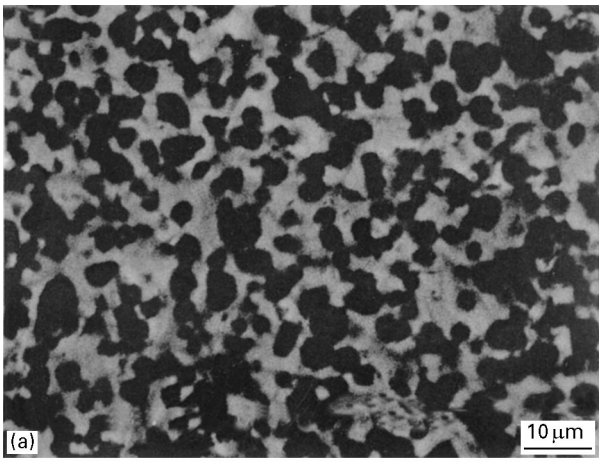

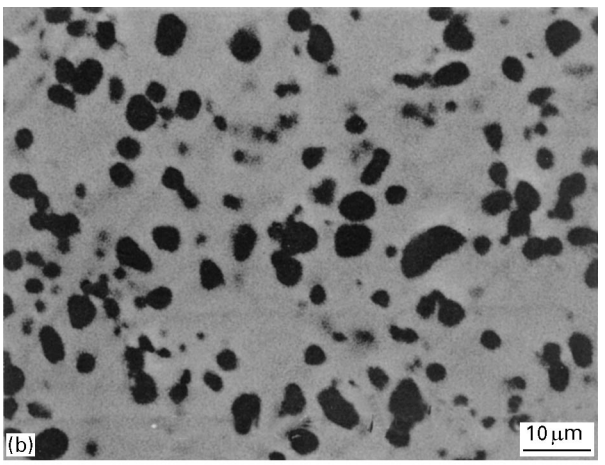

Figure 3 SEM photographs of polished surfaces of (a) composite A and (b) composite B.

3.2. Electrical and mechanical properties of the monolithic composites

The electrical resistivities for the fabricated composites are presented in Table II. The values for $\rho_A (\approx 1 \times 10^{-6}\,\Omega\,m)$ and $\rho_B (\approx 1 \times 10^{9}\,\Omega\,m)$ correspond to those for metallic and insulating materials, respectively. These results can be explained in terms of the "general effective media (GEM)" model [16]. According to this model, the resistivity of an insulating composite whose major component is insulating and whose minor component is a metallic conductor can be represented by the equation,

$$\rho_m = \rho_h(1 - \phi)^3 \quad (1)$$

where ρ_m is the resistivity of the composite, ρ_h the resistivity of the insulating material, and ϕ the volume fraction of the metallic material. When the values of $\rho_h (\approx 10^{10}\,\Omega\,m)$ for $ZrO_2(2Y)$ [18] and $\phi (\approx 0.1945)$ for 30 mol % TiN were substituted into Equation 1, the resistivity ($\rho_{B:GEM}$) of composite B was $\approx 5.2 \times 10^{9}\,\Omega\,m$. Conversely, the resistivity of a composite whose major component is a metallic conductor and whose minor component is an insulating material is described by the equation,

$$\rho_m^* = 1/\{\sigma_h(1 - f)^{3/2}\} \quad (2)$$

where ρ_m^* is the resistivity of the composite, σ_h the conductivity of the metallic material, and f is the volume fraction of the insulating material. The resistivity ($\rho_{A:GEM}$) of composite A, $\approx 1.3 \times 10^{-6}\,\Omega\,m$, was obtained by substituting the values of $\sigma_h (2.5 \times 10^{6}\,\Omega^{-1}\,m^{-1})$ for TiN [17] and $f (\approx 0.5421)$ for 40 mol % $ZrO_2(2Y)$, respectively, into Equation 2. A comparison of the experimental data (Table II) and the theoretical values ($\rho_{A:GEM}$ and $\rho_{B:GEM}$) showed excellent agreement. The textures in both composites are clearly different (Fig. 3(a and b): the TiN (black) grains in composites A and B form continuous and discontinuous phases, respectively, for ZrO_2 (white). Thus, it was found that the electrical resistivities of the composites are strongly dependent on the textures.

TABLE II Electrical and mechanical properties of the composites

Starting powder	Electrical resistivity (Ω m)	Fracture toughness (MPa m$^{1/2}$)	Bending strength (MPa)
A	$\approx 1 \times 10^{-6}$	10.1	1040
B	$\approx 1 \times 10^{9}$	13.0	1180

Table II also lists the fracture toughness and bending strength values of the composites. Composite B has mechanical properties that are superior to those of composite A. This is because composite B has a higher $ZrO_2(2Y)$ content, compared to that of

composite A. The mechanical properties will be discussed later, in connection with those of the laminated materials.

3.3. Electrical and mechanical properties of the laminated materials

The laminated materials with a disk size of ≈ 24 mm in diameter and ≈ 12 mm in thickness (≈ 4 mm thickness per layer) could be successfully fabricated by HIPing. Fig. 4 shows an optical micrograph for the section surface of the material. No cracks in the laminated interfaces were observed. As will be described in more detail later, this is due to the strength of the monolithic composites being greater than the residual stress induced in the interfaces. The bulk and relative densities were 5.82 g cm^{-3} and 99.8% of the theoretical density, respectively.

The electric resistivities, $\rho_\perp$ and $\rho_\parallel$, were measured in the perpendicular and parallel directions, respectively, for the interfaces (Fig. 4). The values derived were $\rho_\perp \approx 1 \times 10^9$ and $\rho_\parallel \approx 1 \times 10^{-6}\,\Omega$m, which agree with those calculated ($\rho_{\perp:\mathrm{GEM}} \approx 1.73 \times 10^9$ and $\rho_{\parallel:\mathrm{GEM}} \approx 1.95 \times 10^{-6}\,\Omega$m) .

Fig. 5 shows the fracture toughness of the material. In layer A, the K_{IC} values, estimated from the length of indentation cracks generated in the parallel direction for the interfaces, decreased from 10.1–8.6 MPa$\cdot$m$^{1/2}$ towards the interfaces, whereas in layer B they increased from 13.1–14 MPa$\cdot$m$^{1/2}$. Data in the perpendicular direction showed results opposite to those described above: the increase (10.1–11.3 MPa$\cdot$m$^{1/2}$) in layer A and a decrease (12.9–11.8 MPa$\cdot$m$^{1/2}$) in layer B. As described earlier, the K_{IC} values of composites A and B were 10.1 and 13 MPa$\cdot$m$^{1/2}$, respectively. These values approximately correspond to the average values obtained in the centre of each layer. These results suggest the presence of a residual stress due to thermal expansion mismatch. The magnitude of the residual stress was estimated using the equation [18],

$$\tau_R = ((\pi)^{1/2}/2)(K_{IC}^0 - K_{IC})/(c)^{1/2} \quad (3)$$

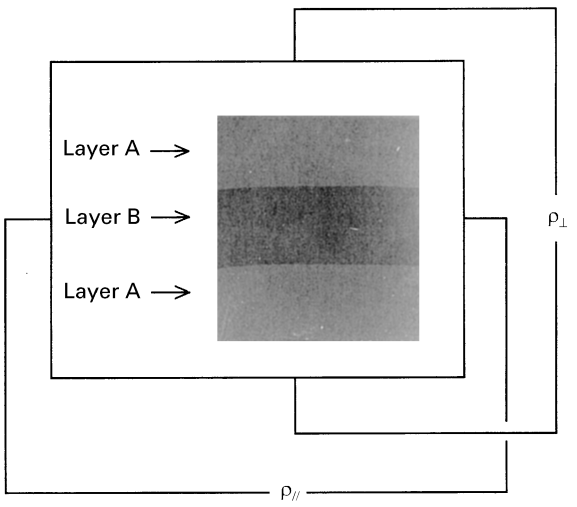

Figure 4 Optical photograph of cross-section of laminated material and schematic showing the measurement of the electrical resistivity.

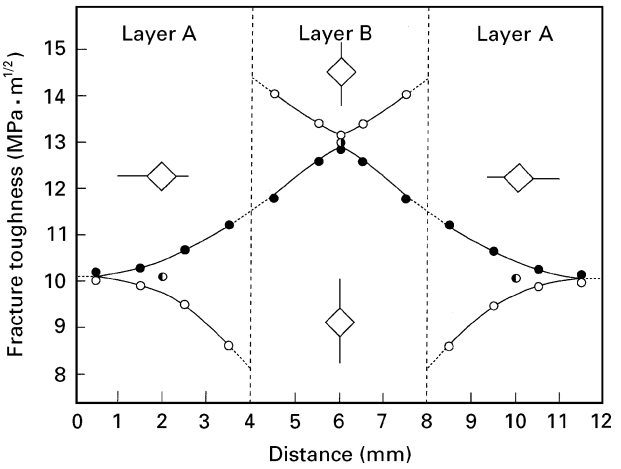

Figure 5 Fracture toughness of laminated material: (○) parallel and (●) perpendicular direction to the interfaces. Symbols (◐) and (◑) show the values of composites A and B, respectively.

where τ_R is the residual stress, K_{IC}^0 and K_{IC} the fracture toughness without and with residual stress, respectively, and c is the length of the cracks generated around indentations. The substitution of the experimental values into Equation 3 yielded a value of $\tau_R \approx$ 150 MPa. The presence of compressive and tensile stress in the laminated materials can be confirmed by the microscopic observation of indentation cracks generated in the perpendicular direction for the interfaces. Crack propagation is suppressed by compressive stress, but promoted by tensile stress. In the present study, the length of cracks in the perpendicular direction for the interfaces in layer A were shorter than those of cracks generated in layer B. These results indicate that the residual stress acted as a compressive stress in layer A and as a tensile stress in layer B. The bending strength, measured in the parallel direction for the interfaces, was 1020 MPa.

4. Conclusions

Little attention has been paid to the fabrication and measurement of properties of laminated materials of composites between ceramics and intermetallics. It has been found that monolithic composites with the compositions of $ZrO_2(2Y)$:TiN = 40:60 (A) and 70:30 (B) mol % show considerable change in their electrical characteristics changing from metallic ($\approx 10^{-6}\,\Omega$m) to insulating ($\approx 10^9\,\Omega$m) behaviour. On the basis of these results, the fabrication of laminated materials consisting of A/B/A layers has been attempted by hot isostatic pressing. Well-densified materials were prepared containing no cracks. The laminates show anisotropic behaviour in their electrical and mechanical properties in the perpendicular and parallel directions to the interfaces. These results highlight possibilities for the development of new materials with intriguing properties.

References

1. A. TSUJI, H. INOUE and K. KOMEYA, *Yōgyō Kyōkai Shi* **82** (1974) 587.

2. H. MITANI, H. NAGAI and M. FUKUYA, *Nippon Kinzoku Gakkaishi* **42** (1987) 582.
3. T. YAMADA, M. SHIMADA and M. KOIZUMI, *Amer. Ceram. Soc. Bull.* **59** (1980) 611.
4. *Idem*, *Yōgyō Kyōkai Shi* **89** (1981) 621.
5. L. THEMELINM and M. BONCOBVA, *Ind. Chem.* **828** (1988) 426.
6. J. H. SELVERIAN and D. O'NEIL, *Thin Solid Films* **235** (1993) 129.
7. K. OKUDA, K. SHIBATA, M. YOSHINAKA, K. HIROTA and O. YAMAGUCHI, *J. Mater. Sci. Lett*. (to be submitted).
8. A. G. EVANS and E. A. CHARLES, *J. Amer. Ceram. Soc*. **59** (1976) 371.
9. K. NIIHARA, N. NAKAHIRA and T. HIRAI, *ibid* **67** (1984) C-13.
10. R. C. GARVIE and P. S. NICHOLSON, *ibid* **55** (1972) 303.
11. R. C. GARVIE, *J. Phys. Chem.* **69** (1965) 1238.
12. K. ENDO, in "New Handbook of High Temperature Compounds (Part 2)" (Nisso Tsūshinsha, Wakayama, 1986) p. 511.
13. F. F. LANGE, *J. Mater. Sci.* **17** (1982) 247.
14. S. HORI, in "Toughening Zirconia" (Uchida Rōkakuho, Tokyo, 1990) p. 139.
15. E. P. INGEL and D. LEWIS III, *J. Amer. Ceram. Soc.* **69** (1986) 325.
16. D. S. McLACHLIN, M. BLASZKIEWICZ and R. E. NEWNHAM, *ibid* **73** (1986) 2187.
17. K. ENDO, in "New Handbook of High Temperature Compounds (Part 1)" (Nisso Tsūshinsha, Wakayama, 1986) p. 355.
18. D. B. MARSHALL and B. R. LAWN, *J. Amer. Ceram. Soc*. **60** (1977) 86.

Received 25 March
and accepted 2 July 1996